Hindawi Publishing Corporation
ISRN Condensed Matter Physics
Volume 2013, Article ID 806374, 9 pages
http://dx.doi.org/10.1155/2013/806374

Research Article

Growth of MoO_3 Films by RF Magnetron Sputtering: Studies on the Structural, Optical, and Electrochromic Properties

S. Subbarayudu, V. Madhavi, and S. Uthanna

Department of Physics, Sri Venkateswara University, Tirupati 517 502, India

Correspondence should be addressed to S. Subbarayudu; srsuguru.phy@gmail.com

Received 18 June 2013; Accepted 28 July 2013

Academic Editors: K. Haenen and L. Pusztai

Copyright © 2013 S. Subbarayudu et al. This is an open access article distributed under the Creative Commons Attribution License, which permits unrestricted use, distribution, and reproduction in any medium, provided the original work is properly cited.

Molybdenum oxide (MoO_3) films were deposited on glass and silicon substrates held at temperature 473 K by RF magnetron sputtering of molybdenum target at various oxygen partial pressures in the range 8×10^{-5}–8×10^{-4} mbar. The deposited MoO_3 films were characterized for their chemical composition, crystallographic structure, surface morphology, chemical binding configuration, and optical properties. The films formed at oxygen partial pressure of 4×10^{-4} mbar were nearly stoichiometric and nanocrystalline MoO_3 with crystallite size of 27 nm. The Fourier transform infrared spectrum of the films formed at 4×10^{-4} mbar exhibited the characteristics vibrational bands of MoO_3. The optical band gap of the films increased from 3.11 to 3.28 eV, and the refractive index increased from 2.04 to 2.16 with the increase of oxygen partial pressure from 8×10^{-5} to 8×10^{-4} mbar, respectively. The electrochromic performance of MoO_3 films formed on ITO coated glass substrates was studied and achieved the optical modulation of about 13% with color efficiency of about 20 cm^2/C.

1. Introduction

Transition metal oxides constitute an interesting group of semiconducting materials because of their technological applications in various fields such as display devices, optical smart windows, electrochromic devices, and gas sensors [1, 2]. Among the transition metal oxides, molybdenum oxide (MoO_3) exhibits interesting structural, chemical, and optical properties. MoO_3 finds application as a cathode material in the development of high energy density solid state microbatteries [3, 4]. It is considered as a chromogenic material since it exhibits electro-, photo-, and gaso chromic (coloration) effects by virtue of which material is of potential for the development of electronic display devices [5]. MoO_3 films in nanocrystalline form also find applications in sensors and lubricants [6]. It is also a promising candidate as a back contact layer for cadmium telluride solar cells in superstrate configuration because of its high work function, which possibly reduces the back contact barrier [7]. Various physical thin film deposition techniques such as thermal evaporation [8, 9], electron beam evaporation [10, 11], pulsed laser deposition [12, 13], and sputtering [14–18] and chemical methods such as electrodeposition [19], chemical vapour deposition [20], spray pyrolysis [21, 22], and sol-gel process [23–25] were employed for the growth of MoO_3 films. Among these films deposition techniques, magnetron sputter deposition is an industrially practiced technique for the growth of oxide films. The physical properties of the sputter deposited MoO_3 films depend critically on the sputter parameters such as oxygen partial pressure, substrate temperature, substrate bias voltage, sputter power, and sputter pressure. The influence of annealing temperature on the structural and optical properties of RF magnetron sputtered of MoO_3 films was earlier reported [18]. In the present investigation, MoO_3 films were formed by RF magnetron sputtering of metallic molybdenum target at different oxygen partial pressures. The effect of oxygen partial pressure on the chemical composition, crystallographic structure, surface morphology and optical properties was studied, and the results were reported.

2. Experimental Details

2.1. Preparation of MoO_3 Thin Films. MoO_3 thin films were deposited onto glass and silicon substrates held at temperature of 473 K by sputtering of pure metallic molybdenum

target in oxygen and argon gas mixture using reactive RF magnetron sputtering technique. Metallic molybdenum target (99.99% pure) with 50 mm diameter and 3 mm thickness was used as sputter target. The sputter chamber was evacuated using a diffusion pump and rotary pump combination to achieve ultimate pressure of 4×10^{-6} mbar. Pressure in the sputter chamber was measured with digital Pirani-Penning gauge combination. Oxygen and argon (99.99% purity) were used as reactive and sputter gases, respectively, for deposition of MoO_3 films. After achieving ultimate pressure, required quantities of oxygen and argon gases were admitted into the sputter chamber through fine controlled needle valves followed by Aalborg mass flow controllers (Model GFC 17). RF power of 150 W was supplied to the sputter target using power supply (Advanced Energy Model ATX-600W) for deposition of the experimental films. The sputter parameters fixed during the growth of the MoO_3 films are given in Table 1.

2.2. Characterization Methods of MoO_3 Thin Films. The MoO_3 films formed at various oxygen partial pressure were characterized by studying their chemical composition, crystallographic structure surface morphology, chemical binding configuration, and optical properties. The thickness of the deposited films was measured with a mechanical Veeco Dektak (Model 150) depth profilometer. The chemical composition of the films was analysed with energy dispersive X-ray analysis (Oxford Instruments Inca Penta FETx3) attached to a scanning electron microscope (Carl Zeiss, model EVO MA15). The crystallographic structure of the films was determined by X-ray diffractometer (Bruker D8 advance diffractometer) using copper K_α radiation with wavelength of $\lambda = 0.15406$ nm. The X-ray diffraction profiles were recorded in the 2θ range 10–60° in steps of 0.05°. The surface morphology of the films was analysed with a scanning electron microscope (Hitachi SEM Model S-400). The chemical binding configuration of the films formed on silicon substrates was analyzed with Fourier transform infrared spectrophotometer (Nicolet Magana IR 750), recorded in the wavenumber range 300–1500 cm^{-1}. The optical transmittance of the films formed on glass substrates was recorded using UV-Vis-NIR double beam spectrophotometer (Perkin Elmer Spectrophotometer Lambda 950) in the wavelength range 300–1500 nm. The electrochromic properties of the MoO_3 films formed at oxygen partial pressure 4×10^{-4} mbar were investigated by three-electrode cell with platinum as a counter electrode, Ag/AgCl as a reference electrode, and the ITO coated MoO_3 films as a working electrode using an EC (Model-CHI 608). The colored and virgin states of the films were measured by UV-Vis-NIR double beam spectrophotometer.

3. Result and Discussion

3.1. Deposition Rate. The thickness of the deposited MoO_3 films determined by using Veeco depth profilometer was 1.3 μm for the films deposited at 8×10^{-5} mbar. As the oxygen partial pressure increased from 2×10^{-4} to 4×10^{-4} mbar, the thickness was increased from 1.8 to 2.2 μm. Further increase of oxygen partial pressure to 8×10^{-4} mbar decreased the thickness to 1.9 μm. The deposition rate of the films was calculated from the measured film thickness and duration of deposition. Figure 1 shows the dependence of deposition rate of MoO_3 films on the oxygen partial pressure. At low oxygen partial pressure of 8×10^{-5} mbar, the deposition rate of MoO_3 films was 11.2 nm/min. The deposition rate gradually increased to 15.5 nm/min with the increase of oxygen partial pressure to 2×10^{-4} mbar and reached 18.3 nm/min for oxygen partial pressure 4×10^{-4} mbar. On further increase of oxygen partial pressure to 8×10^{-4}, the deposition rate decreased to 16.2 nm/min. At low oxygen partial pressures, the increase of deposition rate with the increase of oxygen partial pressure was due to the effective reaction between the metallic molybdenum and oxygen and hence, the increase in the deposition rate. At higher oxygen partial pressures, the chemical reaction between the target surface and the reactive oxygen gas forms molybdenum oxide layer on the target which reduced the deposition rate as observed by Mohamed et al. [26]. Scarminio et al. [5] also noticed such an increase of deposition rate with the increase of oxygen partial pressures and then a decrease at higher oxygen partial pressures in RF sputtered MoO_3 films. The observed decrease in the deposition rate with increase of oxygen partial pressure was due to target poisoning by oxygen atoms, the negative ion impingement on the target surface reduce the film growth [27].

Table 1: Sputter parameters fixed during the growth of the MoO_3 films.

Sputter target	Molybdenum (50 mm diameter and 3 mm thick)
Target to substrate distance	65 mm
Ultimate pressure	4×10^{-6} mbar
Oxygen partial pressure (pO_2)	8×10^{-5}–8×10^{-4} mbar
Substrate temperature (T_s)	473 K
Sputter pressure	4×10^{-2} mbar
Sputter power	150 W
Deposition time	120 min

3.2. Composition Analysis. The chemical composition of the MoO_3 films was determined by using energy dispersive X-ray analysis (EDAX). Figure 2 shows the representative EDAX spectra of the MoO_3 films deposited at oxygen partial pressures of 8×10^{-5} and 4×10^{-4} mbar. The chemical constituents present in the MoO_3 films formed at different oxygen partial pressures are given in Table 2. It is seen that the films formed at low oxygen partial pressure of 8×10^{-5} mbar contained less quantity of oxygen required to form a compound of molybdenum oxide. It revealed that the deposited films contained MoO_3 along with molybdenum. As the oxygen partial pressure increased to 4×10^{-4} mbar, the formed films showed that the atomic ratio of oxygen to molybdenum was 2.98 : 1 which indicated that the stoichiometric MoO_3 films were deposited at 4×10^{-4} mbar. Siciliano et al. [28] also conclude that the atomic ratio of O and Mo was 3 : 1 in

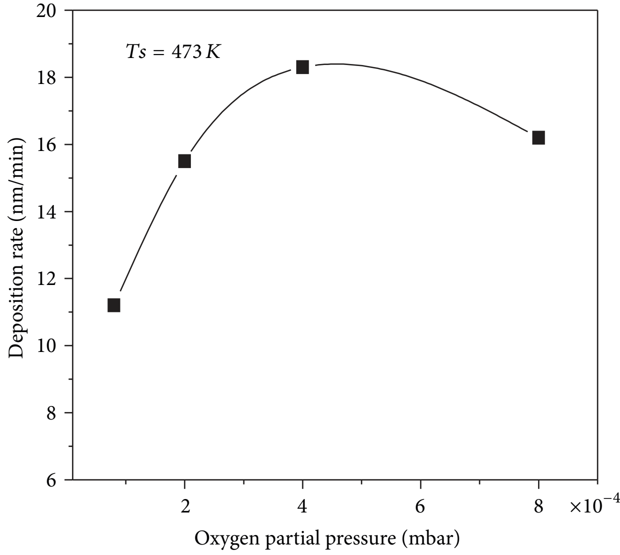

Figure 1: Variation of deposition rate of MoO_3 films with oxygen partial pressure.

the sputter deposited MoO_3 films. It revealed that oxygen partial pressure of 4×10^{-4} mbar is an optimum to achieve stoichiometric MoO_3 films. Further with the increase of oxygen partial pressure to 8×10^{-4} mbar, the atomic ratio of oxygen to molybdenum was found to be 3.03. This indicates that the films were overstoichiometric.

3.3. Structural Studies. Crystallographic structure of the films was analyzed by the X-ray diffraction. Figure 3 shows the X-ray diffraction (XRD) profiles of the MoO_3 films deposited at different oxygen partial pressures. The films formed at low oxygen partial pressure of 8×10^{-5} mbar showed that the X-ray diffraction peak at $2\theta = 26.13^{\circ}$ was related to the (040) reflection of MoO_3. Another peak observed at 38.1° (JCPDS card no. 50-0739) indicated the growth of the mixed phase of MoO_3 and MoO_2. The presence of this (100) peak revealed that the films formed at low oxygen partial pressure of 8×10^{-5} mbar contained the mixed phase of MoO_2 and MoO_3 because of insufficient oxygen present in the sputter chamber to achieve stoichiometric films. When oxygen partial pressure increased to 4×10^{-4} mbar, the films showed a diffraction peak $2\theta = 12.82^{\circ}$ related to the (020) along with (040) reflections of the orthorhombic α-phase of MoO_3 (JCPDS card no. 76-1003) in the amorphous background. Thus, the films formed at low oxygen partial pressure were the mixed phase of MoO_2 and α-MoO_3, and with the increase of oxygen partial pressure the films were transformed into orthorhombic α-phase MoO_3 nanocrystals within the amorphous background. The films formed at higher oxygen partial pressure of 8×10^{-4} mbar showed sharp (020) peak and reduction in the intensity of (040) reflection. Nirupama et al. [29] observed the coexistence of the mixed phase of α- and β-MoO_3 along with elemental molybdenum at oxygen partial pressures $<2 \times 10^{-4}$ mbar and single α-MoO_3 achieved at oxygen partial pressure $\geq 2 \times 10^{-4}$ mbar. Subbarayudu et al. [18] have grown polycrystalline MoO_3 films with the mixed α- and β-phases at oxygen partial pressures 1.9×10^{-1} and 4 mbar and at substrate temperature of 573 K. On increasing the substrate temperature to 923 K, the films were of α-phase MoO_3. Gretener et al. [7] deposited MoO_3 films with 20% of oxygen content at substrate temperature 473 K which consisted of MoO_2 and with 50% of O_2 and at higher substrate temperature of 673 K consisted of MoO_3 associated with Mo_9O_{26} phases. Thus, the grown phases of sputtered MoO_x films strongly depend on oxygen partial pressure prevailed in the sputter chamber during the deposition of the films.

Table 2: Chemical composition analysis of MoO_3 films analyzed by EDAX.

Oxygen partial pressure (mbar)	O (at %)	Mo (at %)	O/Mo
8×10^{-5}	72.4	27.6	2.62
2×10^{-4}	73.2	26.8	2.73
4×10^{-4}	74.8	25.2	2.97
8×10^{-4}	75.2	24.8	3.03

The crystallite size (L) of the films was calculated from the X-ray diffraction reflections by using the Debye-Scherrer relation [30]

$$L = \frac{0.89\lambda}{\beta \cos\theta}, \quad (1)$$

where λ is the wavelength of the X-ray, β the full width at half maximum of diffraction intensity of the diffraction peak measured in radians, and θ the diffraction angle. The crystallite size of the films increased from 24 to 27 nm with the increase of oxygen partial pressure from 2×10^{-4} to 4×10^{-4} mbar, respectively. On further increase of oxygen partial pressure to 8×10^{-4} mbar, the crystallite size of the films decreased to 15 nm.

3.4. Surface Morphology. Figure 4 shows the scanning electron microscope images (SEM) of MoO_3 films formed at different oxygen partial pressures. MoO_3 films deposited at low oxygen partial pressure of 8×10^{-5} mbar consisted of grains on cracking background uniformly distributed on the surface. This grain growth was due to MoO_2 along with MoO_3 at low oxygen partial pressure. When oxygen partial pressure increased to 2×10^{-4} mbar, tiny spherical grain growth started. After that, the films exhibited needle shaped grains uniformly distributed on the surface of substrate at an oxygen partial pressure of 4×10^{-4} mbar. The size of needle shaped grains was about 800 nm long and 120 nm diameter. It is evident that the oxygen partial pressure strongly influenced the surface morphology of the deposited MoO_3 films. Further due to the increase of oxygen partial pressure to 4×10^{-4} mbar, the films showed uniform large size grains which was attributed to the growth of α-phase MoO_3. This uniformity of the films was due to the formation of stoichiometric α-MoO_3. The films grown at higher oxygen partial pressure of 8×10^{-4} mbar showed the fine grain structure. Ramana and Julien [12] found

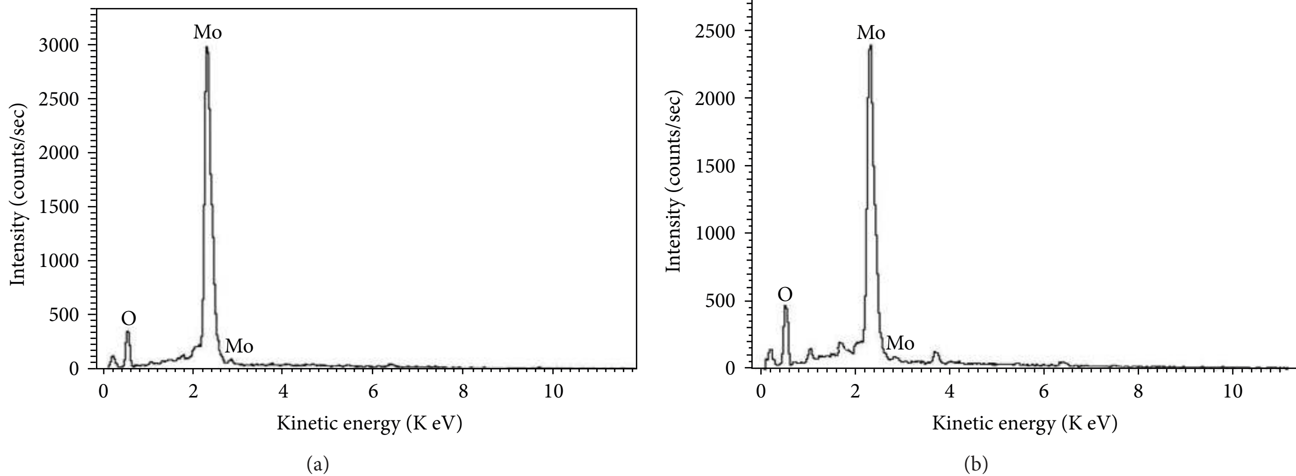

Figure 2: EDAX spectra of MoO_3 films deposited on glass substrates at oxygen partial pressures: (a) 8×10^{-5} mbar and (b) 4×10^{-4} mbar.

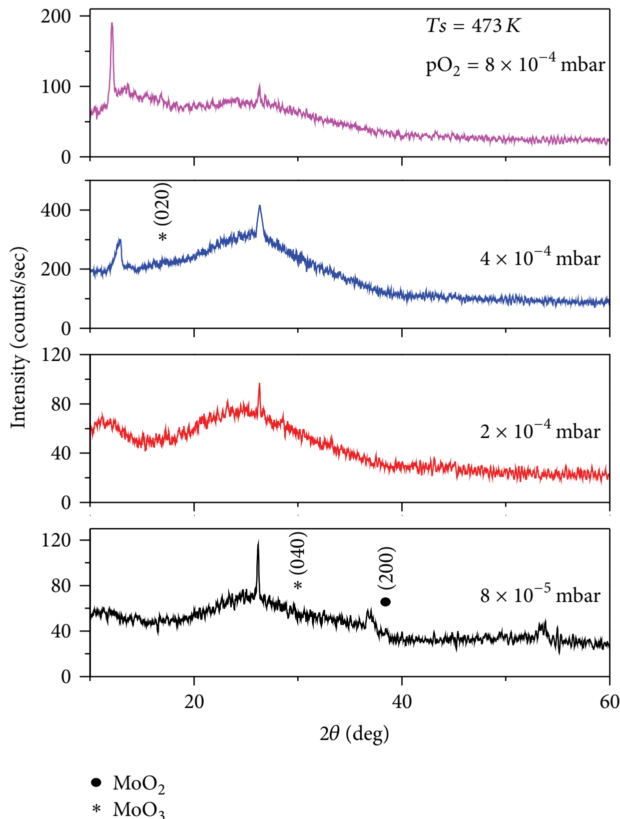

Figure 3: XRD profiles of MoO_3 films deposited on glass substrates at different oxygen partial pressures.

that the MoO_3 films grown at 61% content of oxygen pressure exhibited small grains along with the thin long bars or needle shape grains due to incomplete oxidation.

3.5. Fourier Transform Infrared Spectroscopy. Fourier transform infrared transmittance spectra of MoO_3 films formed on silicon substrates at various oxygen partial pressures were recorded in the wavenumber range 300–1500 cm^{-1} in order to see the chemical binding configuration in the films. Figure 5 shows the Fourier transform infrared transmittance spectra of MoO_3 films formed at different oxygen partial pressures. The FTIR spectra of the films formed at low oxygen partial pressure of 8×10^{-5} mbar contained broadband in the wavenumbers between 600 and 1000 cm^{-1}. The absorption band located at 566 cm^{-1} was due to transverse optical vibrations of Mo-O-Mo, and broadband centered around 794 cm^{-1} was the characteristic bridging vibration of Mo-O. Ivanova et al. [31] observed the transverse optical vibrations of Mo-O-Mo at 558 cm^{-1}. When the oxygen partial pressure increased from 8×10^{-5} to 2×10^{-4} mbar, the FTIR spectra show the absorption bands at 990, 810, 689, and 573 cm^{-1}. The FTIR spectra of the films formed at oxygen partial pressure of 4×10^{-4} mbar showed the absorption bands at about 809, 689, and 572 cm^{-1}. The absorption band observed at 811 cm^{-1} was attributed to the bridging vibrations of Mo = O and indicated that the existence of Mo^{6+} oxidation state was related to α-phase MoO_3. The films deposited at oxygen partial pressure of 8×10^{-4} mbar showed a shift in the absorption bands to 820, 687, and 558 cm^{-1}. The intensity of the absorption band seen at 990 cm^{-1} was associated with the Mo = O stretching vibration. Nirupama et al. [29] noticed that the absorption bands at 894 and 1002 cm^{-1} were corresponding to the growth of α-phase MoO_3 in DC magnetron sputtered MoO_3 films formed at oxygen partial pressure of 4×10^{-4} mbar. These studies confirmed that the oxygen partial pressure of 4×10^{-4} mbar is an optimum to produce the films with stoichiometric α-phase MoO_3.

3.6. Optical Properties. Figure 6 shows the wavelength dependence optical transmittance of the MoO_3 films formed at different oxygen partial pressures. The optical transmittance of the films formed at low oxygen partial pressure of 8×10^{-5} mbar exhibited the average optical transmittance <50% about the fundamental optical

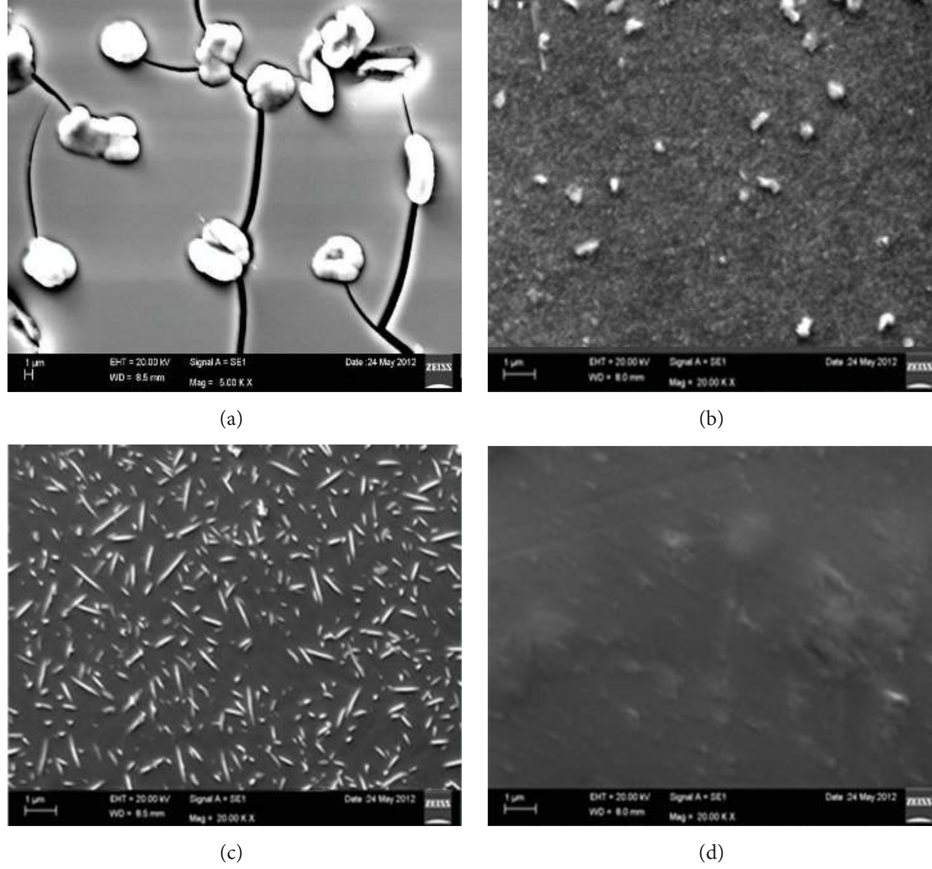

FIGURE 4: SEM images of MoO_3 films formed on glass substrates at oxygen partial pressures: (a) 8×10^{-5} mbar, (b) 2×10^{-4} mbar, (c) 4×10^{-4} mbar, and (d) 8×10^{-4} mbar.

absorption edge. This low optical transmittance at low oxygen partial pressure of 8×10^{-5} mbar was due to the formation of substoinchiometric MoO_3 films which characterize the blue color due to the oxygen ion vacancies [29, 32]. The broadband absorption above wavelength 500 nm was mainly due to the presence of MoO_2 atoms which act as scattering centers of light and hence the decrease in the optical transmittance. As the oxygen partial pressure increased to 4×10^{-4} mbar, the optical transmittance increased to about 85% due to oxygen ion vacancies decrease, and the films transformed into nearly stoichiometric α-MoO_3 films. As the oxygen partial pressure increased to 4×10^{-4} and 8×10^{-4} mbar, there was not much variation in the optical transmittance due to the formation of MoO_3 films as conformed by the EDAX data. The fundamental optical absorption edge in the films was observed in the wavelength range 300–400 nm. The optical absorption edge of the films shifted towards lower wavelength side with the increase of oxygen partial pressure.

The optical absorption coefficient (α) of the films was evaluated from the optical transmittance (T) data using the relation:

$$\alpha = -\left(\frac{1}{t}\right) \ln (T), \quad (2)$$

where t is the film thickness. The optical band gap (E_g) of the films was evaluated from the optical absorption coefficient using the Tauc relation [33] assuming that the direct transition was takes place in these films

$$(\alpha h\upsilon) = A\left(h\upsilon - E_g\right)^{1/2}. \quad (3)$$

The plots of $(\alpha h\upsilon)^2$ versus photon energy ($h\upsilon$) of the films formed at different oxygen partial pressures are shown in Figure 7. The optical band gap of the films was determined from the plot of $(\alpha h\upsilon)^2$ versus photon energy ($h\upsilon$). The extrapolation of the linear portion of plots of $(\alpha h\upsilon)^2$ versus photon energy to $\alpha = 0$ yields the optical band gap of the films. The optical band gap of the MoO_3 films formed at low oxygen partial pressure of 8×10^{-5} was 3.11 eV, and it increased from 3.23 to 3.28 eV with the increase of oxygen partial pressure from 2×10^{-4} to 4×10^{-4} mbar, respectively. On further increase of oxygen partial pressure to 8×10^{-4} mbar, the optical band gap of the films reached 3.35 eV. The low value of the optical band gap of the films formed at low oxygen partial pressures was due to the formation of substoichiometric films, which is the mixed phase of MoO_2 and MoO_3. The films formed at oxygen partial pressure of 4×10^{-4} mbar were of nearly stoichiometric MoO_3 films. These MoO_3 films exhibited the optical band gap of

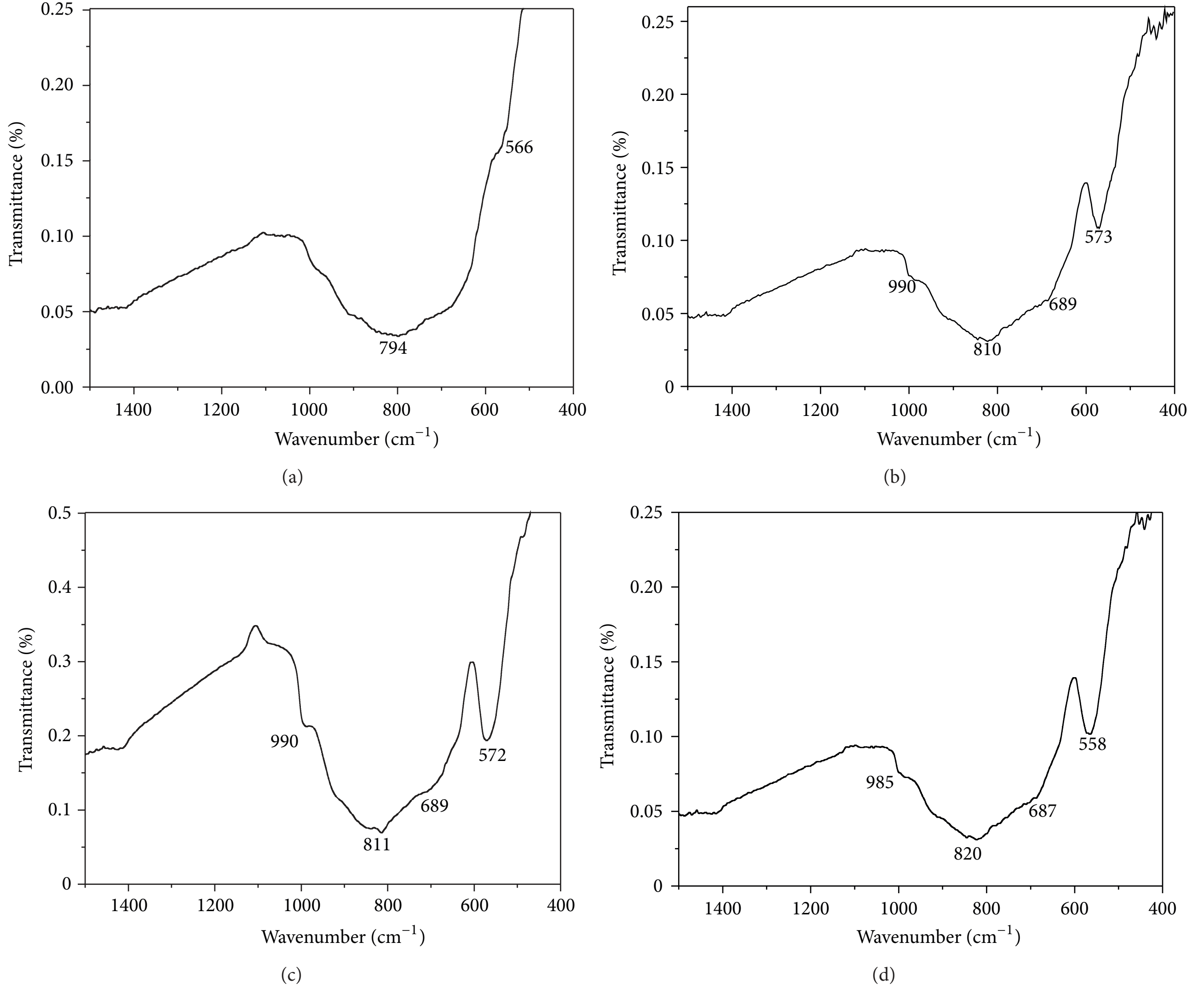

FIGURE 5: FTIR spectra of MoO_3 films formed on silicon substrates at oxygen partial pressures: (a) 8×10^{-5} mbar, (b) 2×10^{-4} mbar (c) 4×10^{-4} mbar, and (d) 8×10^{-4} mbar.

3.28 eV. In the literature, Okumu et al. [34] observed that the optical band gap of the MoO_3 films increased from 3.0 to 3.2 eV with the increase of oxygen partial pressure from 8×10^{-2} to 1.2×10^{-1} mbar in DC magnetron sputtering. Mohamed and Venkataraj [17] noticed that the value of the optical band gap of the films initially increased from 2.64 to 2.69 eV with the increase of oxygen partial pressure from 0.17×10^{-5} to 2.6×10^{-1} mbar and then decreased to 2.67 eV with further increase to 6.4×10^{-1} mbar which was due to the reduction of defect centers and hence improved in stoichiometry. Boudaoud et al. [22] achieved a high optical band gap of 3.35 eV in spray pyrolysis deposited MoO_3 films. It is to be noted that low optical band gap values between 2.60 and 2.70 eV in DC magnetron sputtered [17] and RF magnetron sputtered [35] films were due to the growth of β-MoO_3.

The refractive index (n) of the films was determined from the optical transmittance interference data employing Swanepoel's envelope method used in the following relation [36],

$$n(\lambda) = \left[N + \left(N^2 - n_0^2 n_1^2\right)^{1/2}\right]^{1/2},$$
$$N = 2n_0 n_1 \left[\frac{(T_M - T_m)}{T_M T_m}\right] + \left[\frac{\left(n_0^2 + n_1^2\right)}{2}\right], \tag{4}$$

where T_M and T_m are the optical transmittance maxima and minima and n_0 and n_1 are the refractive indices of air and substrate, respectively. Figure 8 shows the wavelength dependence of refractive index of MoO_3 films formed at different oxygen partial pressures. In general, the refractive index of the MoO_3 films decreased with the increase of wavelength. The refractive index of MoO_3 films (at the wavelength of 500 nm) increased from 2.04 to 2.16 with the increase of oxygen partial pressure from 8×10^{-5} to $8 \times$

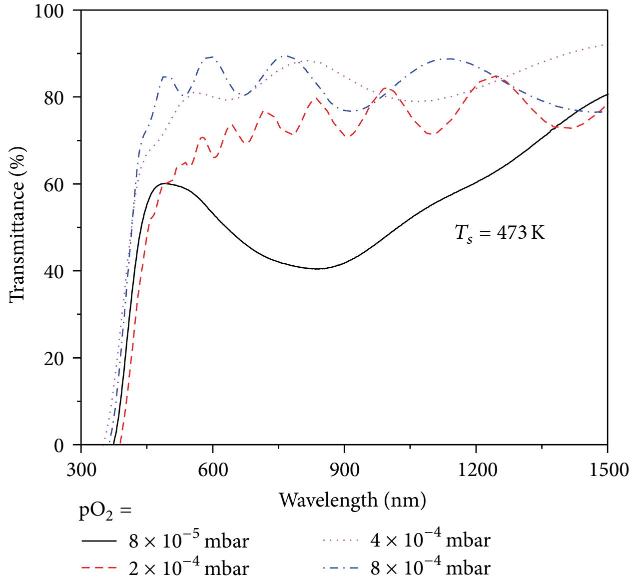

FIGURE 6: Variation of optical transmittance of MoO_3 films deposited on glass substrates at different oxygen partial pressures.

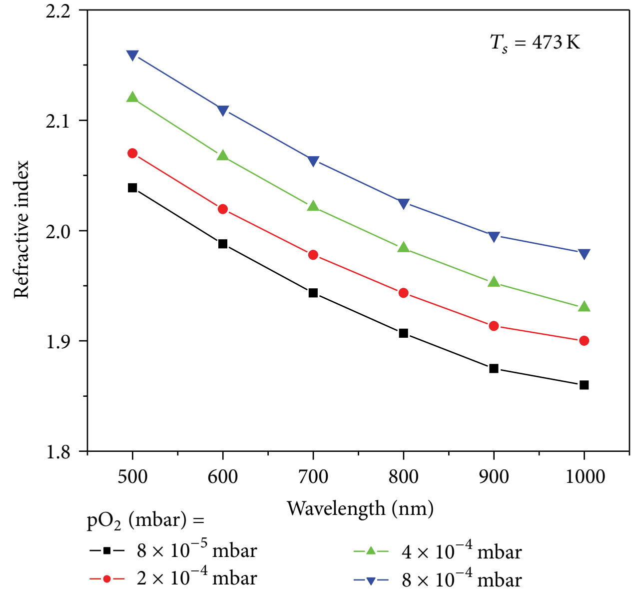

FIGURE 8: Wavelength dependence of refractive index of MoO_3 films deposited on glass substrates at different oxygen partial pressures.

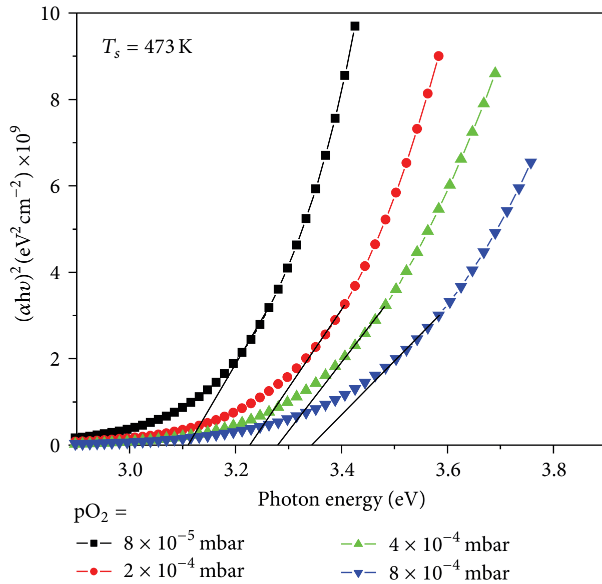

FIGURE 7: Plot of $(\alpha h\nu)^2$ versus photon energy ($h\nu$) of MoO_3 films deposited on glass substrates at different oxygen partial pressures.

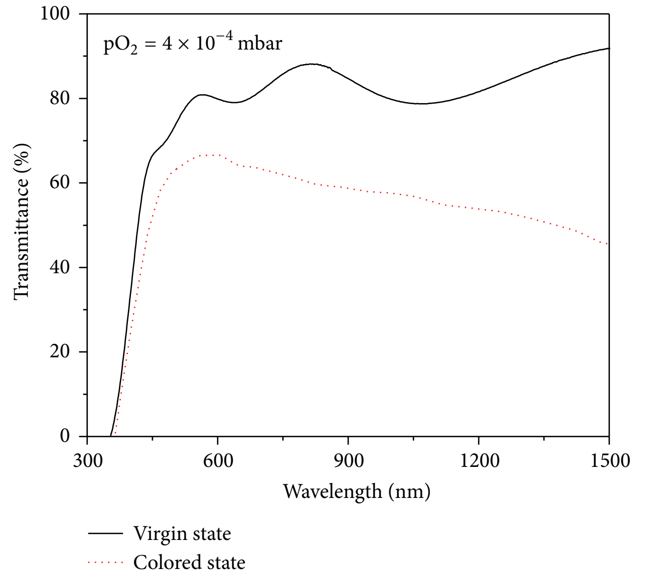

FIGURE 9: Optical transmittance spectra of virgin and colored states of MoO_3 film deposited on glass substrates at oxygen partial pressure of 4 × 10^{-4} mbar.

10^{-4} mbar, respectively. The low value of refractive index at low oxygen partial pressure of 8 × 10^{-5} mbar was due to the presence of MoO_2 along with the MoO_3. The increase in the refractive index at higher oxygen partial pressures was due to the formation of single phase α-MoO_3 and increase in the packing density of the films. It is to be noted from the literature that the refractive index value of 1.8 was achieved by Reyes-Betanzo et al. [37] in thermal evaporation films, while Cárdenas et al. [38] reported 1.9 in pulsed laser deposited films. The refractive index of the DC magnetron sputtered MoO_3 films increased from 2.03 to 2.10 with the increase of substrate temperature from 303 to 573 K [14].

3.7. Electrochromic Properties. In order to study the electrochromic properties, the stoichiometric MoO_3 films were formed on ITO coated glass substrates at oxygen partial pressure of 4 × 10^{-4} mbar. The electrochromic properties of the films were investigated by three-electrode cell, with platinum as a counter electrode, Ag/AgCl as a reference electrode and the indium tin oxide coated MoO_3 films as a

working electrode using an electrochromic cell model (HI 608). The colored and virgin states of the films were measured by UV-Vis-NIR spectrophotometer. In the electrochromism, the coloration is due to the reduction of Mo^{6+} to Mo^{5+} state by insertion of Li^+ ions into the MoO_3 films. In the reverse scan, the virgin state can be achieved by the intercalation charge removed from the films, resulting in the virgin state due to the oxidation of Mo^{5+} to Mo^{6+} state. Figure 9 shows the colored and virgin states of the MoO_3 film formed at oxygen partial pressure of 4×10^{-4} mbar. The optical modulation (ΔT) of the films at 550 nm is about 13%. This optical modulation is mainly dependent on the quantity of Li^+ insertion into the MoO_3 films. The color efficiency (η) at a particular wavelength correlated to the optical contrast; that is, the change in optical density with charges intercalated per unit electrode area and can be expressed with relation [39]:

$$\eta = \frac{\log(T_b/T_c)}{(Q/A)} = \frac{(\Delta OD)}{(Q/A)}, \quad (5)$$

where T_b is the bleaching transmittance, T_c the colored transmittance, Q the charge inserted into the films, and A the area of the films. The color efficiency of the MoO_3 film formed at oxygen partial pressure of 4×10^{-4} mbar was 20 cm^2/C. Lin et al. [40] reported that the coloration efficiency achieved a value of 25.1 cm^2/C in the MoO_3 films formed at room temperature subsequently annealed in air at 573 K.

4. Conclusions

Thin films of molybdenum oxide were deposited on glass and silicon substrates held at temperature of 473 K by RF magnetron sputtering method. The films were formed by sputtering of metallic molybdenum target at various oxygen partial pressures in the range 8×10^{-5}–8×10^{-4} mbar. The energy dispersive X-ray analysis revealed that the films formed at oxygen partial pressure of 4×10^{-4} mbar were nearly stoichiometric. X-ray diffraction studies indicated that the films formed at oxygen partial pressure $<4 \times 10^{-4}$ mbar were the mixed phase of MoO_2 and MoO_3, while those deposited at 4×10^{-4} mbar were single phase α-MoO_3 with crystallite size of 28 nm. Scanning electron microscopic studies revealed that the films grown at 4×10^{-4} mbar exhibited that the grown grains are of needle shape grains with size of about 800 nm. The Fourier transform infrared transmittance spectra indicated the presence of characteristic vibrations of MoO_3 in the films formed at oxygen partial pressure $\geq 4 \times 10^{-4}$ mbar. The optical band gap of the films increased from 3.11 to 3.28 eV, and the refractive index of the films increased from 2.04 to 2.16 with increase of oxygen partial pressure from 8×10^{-5} to 8×10^{-4} mbar, respectively. The electrochromic performance of the stoichiometric MoO_3 films formed on ITO coated glass substrates was studied and achieved the optical modulation of about 13% with color efficiency of about 20 cm^2/C.

References

[1] C. G. Granqvist, *Handbook of Inorganic Electrochromic Materials*, Elsevier, Amsterdam, The Netherlands, 1995.

[2] K. Hinokuma, A. Kishimoto, and T. Kudo, "Coloration dynamics of spin-coated $MoO_3 \bullet nH_2O$ electrochromic films fabricated from peroxo-polymolybdate solution," *Journal of The Electrochemical Society*, vol. 141, pp. 876–879, 1994.

[3] C. Julien, *Lithium Batteries, New Materials, Developments and Perspectives*, Edited by: G. Pistoria, North Holland, Amsterdam, The Netherlands, 1994.

[4] W. Li, F. Cheng, Z. Tao, and J. Chen, "Vapor-transportation preparation and reversible lithium intercalation/deintercalation of α-MoO_3 microrods," *Journal of Physical Chemistry B*, vol. 110, no. 1, pp. 119–124, 2006.

[5] J. Scarminio, A. Lourenço, and A. Gorenstein, "Electrochromism and photochromism in amorphous molybdenum oxide films," *Thin Solid Films*, vol. 302, no. 1-2, pp. 66–70, 1997.

[6] A. K. Prasad, D. J. Kubinski, and P. I. Gouma, "Comparison of sol-gel and ion beam deposited MoO_3 thin film gas sensors for selective ammonia detection," *Sensors and Actuators B*, vol. 93, no. 1–3, pp. 25–30, 2003.

[7] C. Gretener, J. Perrenouda, L. Kranza et al., "Development of MoOx thin films as back contact buffer for CdTe solar cells in substrate configuration," *Thin Solid Films*, vol. 535, pp. 193–197, 2013.

[8] T. S. Sian and G. B. Reddy, "Stoichiometric amorphous MoO_3 films: a route to high performance electrochromic devices," *Journal of Applied Physics*, vol. 98, no. 2, Article ID 026104, 2005.

[9] W.-Q. Yang, Z.-R. Wei, X.-H. Zhu, and D.-Y. Yang, "Strong influence of substrate temperature on the growth of nanocrystalline MoO_3 thin films," *Physics Letters A*, vol. 373, no. 43, pp. 3965–3968, 2009.

[10] R. Sivakumar, R. Gopalakrishnan, M. Jayachandran, and C. Sanjeeviraja, "Characterization on electron beam evaporated α-MoO_3 thin films by the influence of substrate temperature," *Current Applied Physics*, vol. 7, no. 1, pp. 51–59, 2007.

[11] V. K. Sabhapathi, O. M. Hussain, S. Uthanna et al., "A.c. conductivity studies on $Al/MoO_3/Al$ sandwich structures," *Materials Science and Engineering B*, vol. 32, no. 1-2, pp. 93–97, 1995.

[12] C. V. Ramana and C. M. Julien, "Chemical and electrochemical properties of molybdenum oxide thin films prepared by reactive pulsed-laser assisted deposition," *Chemical Physics Letters*, vol. 428, no. 1–3, pp. 114–118, 2006.

[13] C. V. Ramana, V. V. Atuchin, V. G. Kesler et al., "Growth and surface characterization of sputter-deposited molybdenum oxide thin films," *Applied Surface Science*, vol. 253, no. 12, pp. 5368–5374, 2007.

[14] S. Uthanna, V. Nirupama, and J. F. Pierson, "Substrate temperature influenced structural, electrical and optical properties of dc magnetron sputtered MoO_3 films," *Applied Surface Science*, vol. 256, no. 10, pp. 3133–3137, 2010.

[15] K. Srinivasarao, B. Rajini Kanth, and P. K. Mukhopadhyay, "Optical and IR studies on r.f. magnetron sputtered ultra-thin MoO_3 films," *Applied Physics A*, vol. 96, no. 4, pp. 985–990, 2009.

[16] I. Navas, R. Vinodkumar, K. J. Lethy et al., "Growth and characterization of molybdenum oxide nanorods by RF magnetron sputtering and subsequent annealing," *Journal of Physics D*, vol. 42, no. 17, Article ID 175305, 2009.

[17] S. H. Mohamed and S. Venkataraj, "Thermal stability of amorphous molybdenum trioxide films prepared at different

oxygen partial pressures by reactive DC magnetron sputtering," *Vacuum*, vol. 81, no. 5, pp. 636–643, 2007.

[18] S. Subbarayudu, V. Madhavi, and S. Uthanna, "Post-deposition annealing controlled structural and optical properties of RF magnetron sputtered MoO_3 films," *Advanced Materials Letters*, vol. 4, no. 8, pp. 637–642, 2013.

[19] R. S. Patil, M. D. Uplane, and P. S. Patil, "Structural and optical properties of electrodeposited molybdenum oxide thin films," *Applied Surface Science*, vol. 252, no. 23, pp. 8050–8056, 2006.

[20] T. Itoh, I. Matsubara, W. Shin, N. Izu, and M. Nishibori, "Preparation of layered organic-inorganic nanohybrid thin films of molybdenum trioxide with polyaniline derivatives for aldehyde gases sensors of several tens ppb level," *Sensors and Actuators B*, vol. 128, no. 2, pp. 512–520, 2008.

[21] H. M. Martinez, J. Torres, L. D. Lopez Correno, and M. E. Rodriguez-Garcia, "Effect of the substrate temperature on the physical properties of molybdenum tri-oxide thin films obtained through the spray pyrolysis technique," *Materials Characterization*, vol. 75, pp. 184–193, 2013.

[22] L. Boudaoud, N. Benramdane, R. Desfeux, B. Khelifa, and C. Mathieu, "Structural and optical properties of MoO_3 and V_2O_5 thin films prepared by Spray Pyrolysis," *Catalysis Today*, vol. 113, no. 3-4, pp. 230–234, 2006.

[23] C.-S. Hsu, C.-C. Chan, H.-T. Huang, C.-H. Peng, and W.-C. Hsu, "Electrochromic properties of nanocrystalline MoO_3 thin films," *Thin Solid Films*, vol. 516, no. 15, pp. 4839–4844, 2008.

[24] J. Kaur, V. D. Vankar, and M. C. Bhatnagar, "Effect of MoO_3 addition on the NO_2 sensing properties of SnO_2 thin films," *Sensors and Actuators B*, vol. 133, no. 2, pp. 650–655, 2008.

[25] M. Dhanasankar, K. K. Purushothaman, and G. Muralidharan, "Effect of temperature of annealing on optical, structural and electrochromic properties of sol-gel dip coated molybdenum oxide films," *Applied Surface Science*, vol. 257, no. 6, pp. 2074–2079, 2011.

[26] S. H. Mohamed, O. Kappertz, J. M. Ngaruiya, T. P. Leervad Pedersen, R. Drese, and M. Wuttig, "Correlation between structure, stress and optical properties in direct current sputtered molybdenum oxide films," *Thin Solid Films*, vol. 429, no. 1-2, pp. 135–143, 2003.

[27] M. S. Oh, B. S. Yang, J. H. Lee et al., "Improvement of electrical and optical properties of molybdenum oxide thin films by ultralow pressure sputtering method," *Journal of Vacuum Science & Technology A*, vol. 30, no. 3, Article ID 031501, 7 pages, 2012.

[28] T. Siciliano, A. Tepore, E. Filippo, G. Micocci, and M. Tepore, "Characteristics of molybdenum trioxide nanobelts prepared by thermal evaporation technique," *Materials Chemistry and Physics*, vol. 114, no. 2-3, pp. 687–691, 2009.

[29] V. Nirupama, K. R. Gunasekhar, B. Sreedhar, and S. Uthanna, "Effect of oxygen partial pressure on the structural and optical properties of dc reactive magnetron sputtered molybdenum oxide films," *Current Applied Physics*, vol. 10, no. 1, pp. 272–278, 2010.

[30] B. D. Cullity, *Elements of X-Ray Diffraction*, Addison Wesley, London, UK, 2nd edition, 1978.

[31] T. Ivanova, K. A. Gesheva, and A. Szekeres, "Structure and optical properties of CVD molybdenum oxide films for electrochromic application," *Journal of Solid State Electrochemistry*, vol. 7, no. 1, pp. 21–24, 2002.

[32] V. K. Sabhapathi, O. M. Hussain, P. S. Reddy et al., "Optical absorption studies in molybdenum trioxide thin films," *Physica Status Solidi A*, vol. 148, no. 1, pp. 167–173, 1995.

[33] J. Tauc, *Amourphous and Liquid Semiconductor*, Plenum Press, New York, NY, USA, 1974.

[34] J. Okumu, F. Koerfer, C. Salinga, T. P. Pedersen, and M. Wuttig, "Gasochromic switching of reactively sputtered molybdenumoxide films: a correlation between film properties and deposition pressure," *Thin Solid Films*, vol. 515, no. 4, pp. 1327–1333, 2006.

[35] N. Miyata and S. Akiyoshi, "Preparation and electrochromic properties of rf-sputtered molybdenum oxide films," *Journal of Applied Physics*, vol. 58, no. 4, pp. 1651–1655, 1985.

[36] R. Swanepoel, "Determination of the thickness and optical constants of amorphous silicon," *Journal of Physics E*, vol. 16, no. 12, pp. 1214–1222, 1983.

[37] C. Reyes-Betanzo, J. L. Herrera-Pérez, G. H. Cocoletzi, and O. Zelaya-Angel, "Refractive index of colored films of molybdenum trioxide," *Journal of Applied Physics*, vol. 88, no. 1, pp. 223–226, 2000.

[38] R. Cárdenas, J. Torres, and J. E. Alfonso, "Optical characterization of MoO_3 thin films produced by continuous wave CO_2 laser-assisted evaporation," *Thin Solid Films*, vol. 478, no. 1-2, pp. 146–151, 2005.

[39] C. G. Granqvist, "Electrochromic tungsten oxide films: review of progress 1993-1998," *Solar Energy Materials and Solar Cells*, vol. 60, no. 3, pp. 201–262, 2000.

[40] S.-Y. Lin, C.-M. Wang, K.-S. Kao, Y.-C. Chen, and C.-C. Liu, "Electrochromic properties of MoO_3 thin films derived by a sol-gel process," *Journal of Sol-Gel Science and Technology*, vol. 53, no. 1, pp. 51–58, 2010.

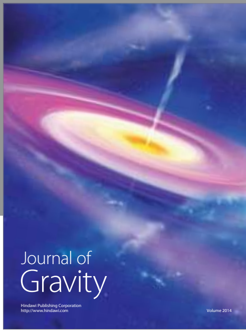
Journal of
Gravity

Journal of
Photonics

The Scientific
World Journal

Journal of
Soft Matter
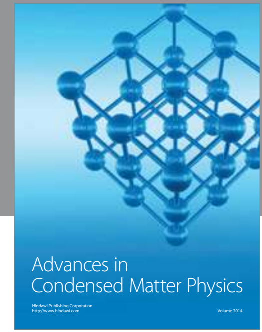
Advances in
Condensed Matter Physics

Journal of
Fluids

Hindawi
Submit your manuscripts at
http://www.hindawi.com
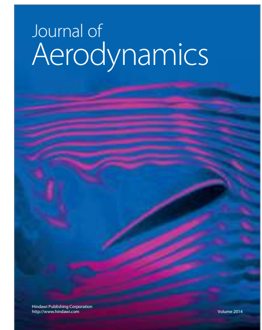
Journal of
Aerodynamics

International Journal of
Statistical Mechanics

International Journal of
Optics
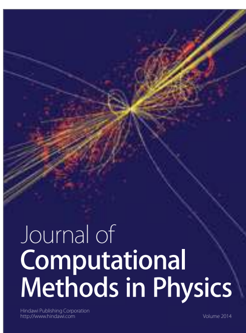
Journal of
Computational
Methods in Physics
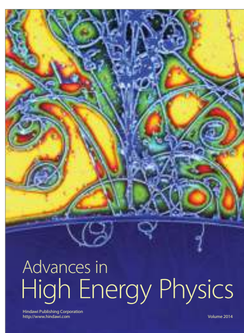
Advances in
High Energy Physics

Journal of
Thermodynamics
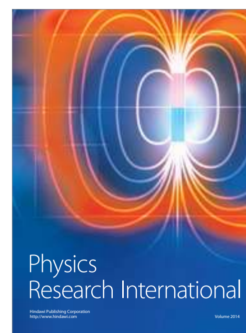
Physics
Research International
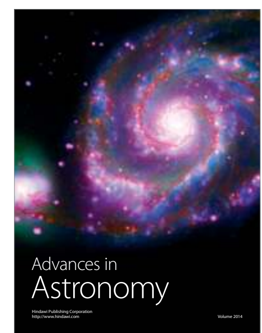
Advances in
Astronomy

Journal of
Solid State Physics

Journal of
Astrophysics

International Journal of
Superconductivity

Journal of
Biophysics
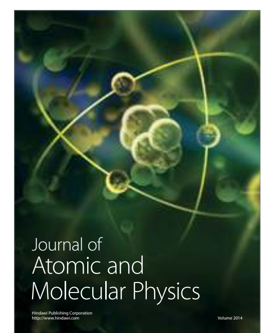
Journal of
Atomic and
Molecular Physics